Konrad-Zuse-Zentrum
für Informationstechnik Berlin

Takustraße 7
D-14195 Berlin-Dahlem
Germany

JENS BURGSCHWEIGER, BERND GNÄDIG, AND
MARC C. STEINBACH

Nonlinear Programming Techniques for Operative Planning in Large Drinking Water Networks

ZIB-Report 05-31 (July 2005)

NONLINEAR PROGRAMMING TECHNIQUES FOR OPERATIVE PLANNING IN LARGE DRINKING WATER NETWORKS

JENS BURGSCHWEIGER, BERND GNÄDIG, AND MARC C. STEINBACH

ABSTRACT. Mathematical decision support for operative planning in water supply systems is highly desirable but leads to very difficult optimization problems. We propose a nonlinear programming approach that yields practically satisfactory operating schedules in acceptable computing time even for large networks. Based on a carefully designed model supporting gradient-based optimization algorithms, this approach employs a special initialization strategy for convergence acceleration, special minimum up and down time constraints together with pump aggregation to handle switching decisions, and several network reduction techniques for further speed-up. Results for selected application scenarios at Berliner Wasserbetriebe demonstrate the success of the approach.

0. INTRODUCTION

Stringent requirements on cost effectiveness and environmental compatibility generate an increased demand for model-based decision support tools in designing and operating municipal water supply systems. This paper is concerned with minimum cost operation of drinking water networks. Operative planning in water networks is difficult: A sound mathematical model leads to nonlinear mixed-integer optimization, which is currently impractical for large water supply networks as in Berlin. Because of the enormous complexity of the task, early mathematical approaches typically rely on substantially simplified network hydraulics (by dropping all nonlinearities or addressing the static case, for instance) [15, 16, 18, 21, 32, 41, 50, 51], which is often unacceptable in practice. Other authors employ discrete dynamic programming [9, 10, 12, 38, 39, 53], which is mathematically sound but only applicable to small networks unless specific properties can be exploited to increase efficiency. Optimization methods based on nonlinear models (mostly for the pumps only) are reported in [3, 11, 14, 29, 45]. These approaches employ computationally expensive meta-heuristics or suffer from inefficient coupling of gradient-based optimization with non-smooth simulation by existing network hydraulics software, such as EPANET [44]. Other topics in water management include network design [31, 47, 52], on-line control [36, 43], state estimation [1], and contamination detection [33]. More loosely related recent work addresses modeling and optimization for networks of irrigation and sewage canals or for gas networks, see, e.g., [17, 20, 27, 28, 34, 40, 49]. Previous efforts toward minimum cost operation at Berliner Wasserbetriebe include:

- experiments with various optimization models and methods [4, 5],
- a first nonlinear programming (NLP) model developed under GAMS [24],
- numerical results for a substantially reduced network graph using (under GAMS) the SQP codes CONOPT, SNOPT, and the augmented Lagrangian code MINOS.

The main goal of the joint work reported here was the development of a decision support tool suitable for routine application, to be implemented as an optimization module within the new operational control system of Berliner Wasserbetriebe. The approach was restricted to the framework sketched above: a pure NLP model (no integer variables),

2000 *Mathematics Subject Classification.* 65K10, 90C06, 90C11, 90C30, 90C35, 90C90.

Key words and phrases. Water supply, large-scale nonlinear programming, convergence acceleration, discrete decisions, network reduction.

TABLE 1. Notation.

Symbol	Explanation	Value	Unit
Q	Volumetric flow rate in arcs		m^3/s
D	Demand flow rate at junctions		m^3/s
H	Pressure potential at nodes (head)		m
ΔH	Pressure increase at pumps, decrease at valves		m
L	Pipe length		m
d	Pipe diameter (bore)		m
k	Pipe roughness		m
A	Pipe cross-sectional area		m^2
λ	Pipe friction coefficient		–
r	Pipe hydraulic loss coefficient		s^2/m^5
ρ	Water density	1000	kg/m^3
g	Gravity constant	9.81	m/s^2

the GAMS modeling environment, and the listed NLP solvers. Criteria for applicability are speed (response time), reliability, and practicability. Our mathematical developments toward these goals are based on two internal studies [25, 26] and can be coarsely categorized into modeling techniques (reported in [6]) and nonlinear programming techniques (reported here). Basic modeling techniques include, in particular, a globally smooth and asymptotically correct approximation of the hydraulic pressure loss in pipes, and suitably aggregated models for collections of pumps that operate in parallel. The NLP techniques include, among others, a sequential linear programming type initialization procedure for the nonlinear iteration, special constraints that ensure minimum up and down times in pump operation, and various network reduction techniques. Together with pump aggregation, the up and down time constraints permit the handling of discrete decisions (pump switching) without introducing binary variables. Following the NLP-based network-wide optimization, nonlinear mixed-integer models are solved locally at each waterworks.

We start by summarizing the component models of all network elements in Section 1, followed by the overall NLP model. In Section 2, the smoothing and SLP initialization are discussed along with further convergence enhancement techniques. Section 3 is devoted to combinatorial issues, particularly the prevention of undesired pump switching. Several network reduction strategies are then developed in Section 4 with special emphasis on suitable smoothing of the hydraulic friction loss. Finally, Section 5 presents selected application scenarios at Berliner Wasserbetriebe to demonstrate the success of our approach.

1. OPTIMIZATION MODEL

To keep the paper self-contained, we first summarize the basic nonlinear programming model developed in [6]. This model covers the physical and technical network behavior. Later on we will add further constraints and develop graph reduction techniques to achieve desired solution behavior and to enable efficient treatment by the chosen standard NLP solvers. The basic notation used in our model is given in Table 1.

1.1. **Optimization Horizon.** We consider a planning period of length T in discrete time, $t = 1, 2, \dots, T$, with initial conditions at $t = 0$. The subinterval $(t - 1, t)$ will be referred to as period t and has physical length Δt. At Berliner Wasserbetriebe, the planning period represents the following day, partitioned into 24 one-hour time-steps.

1.2. **Network Topology.** The network model is based on a directed graph $G = (\mathcal{N}, \mathcal{A})$ whose node set represents junctions, reservoirs, and tanks,

$$\mathcal{N} = \mathcal{N}_{jc} \cup \mathcal{N}_{rs} \cup \mathcal{N}_{tk},$$

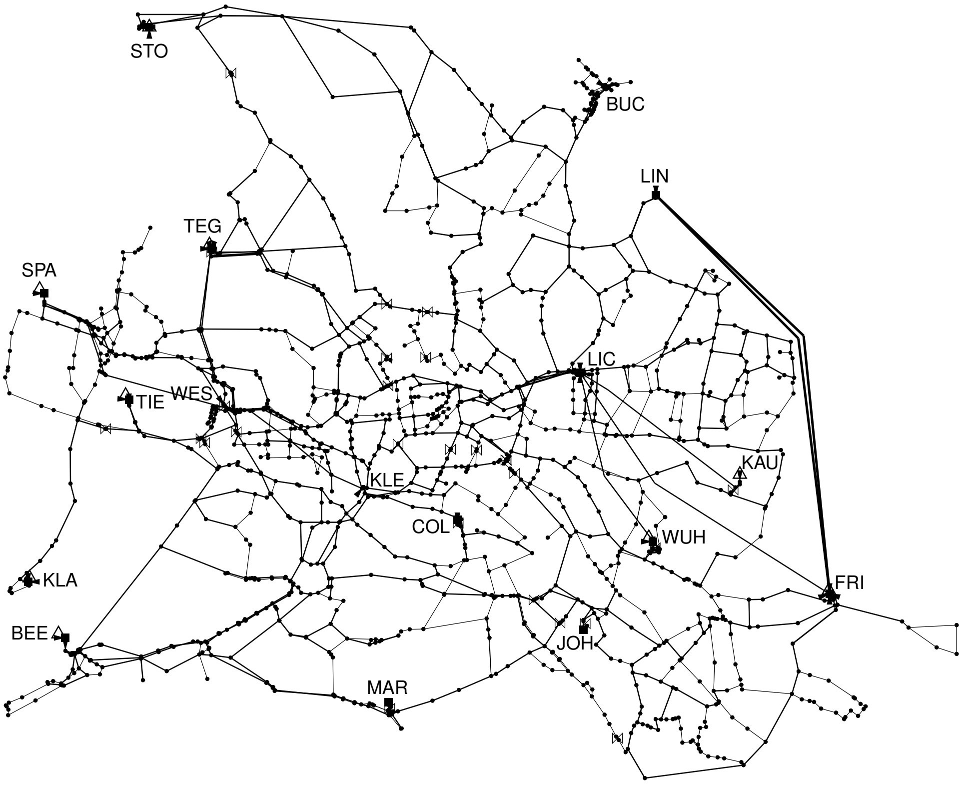

FIGURE 1. Main distribution network of Berliner Wasserbetriebe

and whose arc set represents pipes, pumps, and gate valves,

$$\mathcal{A} = \mathcal{A}_{\text{pi}} \cup \mathcal{A}_{\text{pu}} \cup \mathcal{A}_{\text{vl}}.$$

The set of pumps consists of raw water pumps and pure water pumps, $\mathcal{A}_{\text{pu}} = \mathcal{A}_{\text{pr}} \cup \mathcal{A}_{\text{pp}}$.

We denote arcs as $a \in \mathcal{A}$ or, with tail and head $i, j \in \mathcal{N}$, as $ij \in \mathcal{A}$. A flow from i to j is positive, from j to i negative. Some arcs (such as pumps) may not admit negative flow.

Figure 1 illustrates the *main network* of Berliner Wasserbetriebe, with 1481 nodes and 1935 arcs. Earlier investigations were based on a small *test configuration* with 144 nodes and 192 arcs; cf. [6].

1.3. **Pressure and Flow.** Due to the incompressibility of water, pressure p can equivalently be expressed as an elevation difference Δh,

$$\Delta h = \frac{p}{g\rho}.$$

We thus measure pressure by the *head* H, which is the sum of the actual geodetic elevation and of the elevation difference corresponding to the hydrostatic or hydraulic pressure.

Pressure variables H_{jt} with upper and lower bounds $H^{\pm}_{jt}$ are associated with every node $j \in \mathcal{N}$ and time period t. Most of the bounds are static, i.e., $H^{\pm}_{jt} = H^{\pm}_{j}$ for $t = 1, \dots, T$. Network-wide default bounds, $H^- = 20\,\text{m}$ and $H^+ = 125\,\text{m}$, keep the NLP iterates within reasonable physical limits. Tighter bounds are specified where appropriate.

Volumetric flow rates Q_{at} with bounds $Q^{\pm}_{at}$ are associated with every arc $a \in \mathcal{A}$. Here we use default values $Q^{\pm} = \pm 10\,\text{m}^3/\text{s}$, and again tighter bounds where appropriate.

Further variables are the controlled pressure increase in pumps and decrease in valves, ΔH_{at}, $a \in \mathcal{A}_{\text{pu}} \cup \mathcal{A}_{\text{vl}}$, with bounds $\Delta H^{\pm}_{at}$. The default values are $\Delta H^{-}_{at} = 0\,\text{m}$ in pumps, $\Delta H^{-}_{at} = -125\,\text{m}$ in valves, and $\Delta H^{+}_{at} = 125\,\text{m}$ in both cases.

1.4. **Junction Model.** At the junctions $j \in \mathcal{N}_{jc}$, we have flow balance equations involving the predicted consumption demands D_{jt},

$$c_{jt}^{\text{flow}} \triangleq \sum_{i:\, ij \in \mathcal{A}} Q_{ijt} - \sum_{k:\, jk \in \mathcal{A}} Q_{jkt} - D_{jt} = 0. \tag{1}$$

Tightened pressure bounds $H_{jt}^{\pm}$ are imposed at all waterworks outlets, and at predefined *pressure measurement points* where sensors are installed to monitor the network state.

1.5. **Reservoir Model.** Reservoirs $j \in \mathcal{N}_{rs}$ behave like unlimited sources of raw water. Here the pressure has a known constant value $\bar{H}_j$,

$$c_{jt}^{\text{head}} \triangleq H_{jt} - \bar{H}_j = 0,$$

and no further constraints need to be satisfied since the amounts of water extracted from the reservoirs are bounded by limits associated with the raw water pumps; see Section 1.8.

1.6. **Tank Model.** Flow balance equations at the tanks $j \in \mathcal{N}_{tk}$ involve tank inflows E_{jt},

$$c_{jt}^{\text{flow}} \triangleq \sum_{i:\, ij \in \mathcal{A}} Q_{ijt} - \sum_{k:\, jk \in \mathcal{A}} Q_{jkt} - E_{jt}(H_{j,t-1}, H_{jt}) = 0. \tag{2}$$

A conceptual tank usually consists of several hydraulically communicating physical tanks that may be temporarily unavailable. Using binary variables $Y_{j\nu t} \in \{0, 1\}$ to represent the (externally prescribed) availability profiles, the tank inflows can be written

$$E_{jt}(H_{j,t-1}, H_{jt}) = \frac{1}{\Delta t} \sum_{\nu=1}^{N_a} Y_{j\nu t} \Delta V_{j\nu}(H_{j,t-1}, H_{jt}),$$

where $\Delta V_{j\nu}$ denotes the change of the filling volume of tank $j\nu$ during period t,

$$\Delta V_{j\nu}(H_{j,t-1}, H_{jt}) = \int_{H_{j,t-1}}^{H_{jt}} A_{j\nu}(h - z_j)\, dh.$$

Here the cross-sectional tank area $A_{j\nu}$ depends on the filling height above the tank floor z_j. The pressure variables H_{jt} represent the tank filling level, with static bounds $H_j^{\pm}$ determined by dry run and overflow.

1.7. **Pipe Model.** In every pipe, $a = ij \in \mathcal{A}_{pi}$, hydraulic friction causes a pressure loss,

$$c_{at}^{\text{loss}} \triangleq H_{jt} - H_{it} + \Delta H_a(Q_{at}) = 0. \tag{3}$$

The flow dependence of the pressure loss is usually expressed as

$$\Delta H_a(Q_{at}) = r_a(Q_{at}) Q_{at} |Q_{at}|, \tag{4}$$

where the hydraulic loss coefficient $r_a(Q_{at})$ depends on the pipe length and diameter,

$$r_a(Q_{at}) = \frac{L_a}{2 g d_a A_a^2} \lambda_a(Q_{at}) = \frac{8 L_a}{\pi^2 g d_a^5} \lambda_a(Q_{at}), \tag{5}$$

and the friction coefficient $\lambda_a(Q_{at})$ depends on the flow rate and on the pipe roughness k_a. A highly accurate model for λ_a is based on the laws of Hagen–Poiseuille (laminar flow) and Prandtl–Colebrook (turbulent flow); we call this the *HP-PC model*. A much simpler, flow-independent formula is the law of Prandtl–Kármán for rough pipes (*PKr model*),

$$\lambda_a^{\text{PKr}} = \left(2 \log \frac{k_a/d_a}{3.71} \right)^{-2}, \quad r_a^{\text{PKr}} = \frac{8 L_a}{\pi^2 g d_a^5} \lambda_a^{\text{PKr}}, \tag{6}$$

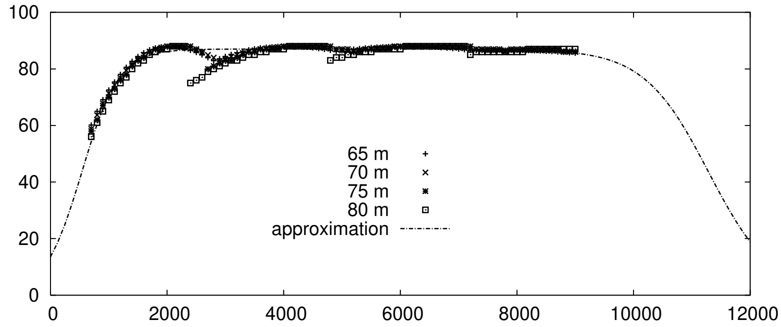

FIGURE 2. Efficiency of aggregated pumps under optimal configuration

which provides a valid approximation for highly turbulent flow, that is, large Q_{at}. In [6] we have proposed a globally smooth, asymptotically correct approximation for ΔH_a,

$$\Delta H_a^{\mathrm{PKrs}}(Q) = r_a^{\mathrm{PKr}} \left(\sqrt{Q^2 + a_a^2} + b_a + \frac{c_a}{\sqrt{Q^2 + d_a^2}} \right) Q. \tag{7}$$

This formula shares the leading coefficient with the PKr model, $\Delta H_a^{\mathrm{PKr}}(Q) = r_a^{\mathrm{PKr}} Q|Q|$. We call it the *smoothed PKr model (PKrs model)*; for more details see [6] and Section 2.1.

1.8. **Pump Model.** Every pump $a = ij \in \mathcal{A}_{\mathrm{pu}}$ increases the pressure by some nonnegative amount ΔH_{at},

$$c_{at}^{\mathrm{diff}} \triangleq H_{jt} - H_{it} - \Delta H_{at} = 0. \tag{8}$$

As with the tanks, our conceptual pumps generally consist of several physical pumps operated in parallel. This applies to raw water pumps and to pure water pumps (at the outlets of waterworks and pumping stations) and leads to a largely simplified modeling based on an approximation of the combined efficiency; see [6, §2.8]. The quality generally increases with the number of pumps in the collection, although the approximation can also be applied to single pumps.

Large collections of pumps can be assumed to run with constant energy demand per m^3, w_a, entering the cost model (15). At Berliner Wasserbetriebe this applies to raw water pumping in all nine waterworks, whose 620 pumps operate in groups of 14 to 170 units.

For small collections of pumps (all pure water outlets at Berliner Wasserbetriebe) the aggregate efficiency model must respect the flow dependence. Under the assumption that the optimal configuration of pumps is selected for every flow value, the efficiency can be approximated as

$$\eta_a(Q_{at}) = \eta_a^{\max} \left(\frac{1}{\phi_a^-(Q_{at})} - \frac{1}{\phi_a^+(Q_{at})} \right) + 0.001, \tag{9}$$

where

$$\phi_a^{\pm}(Q) = 1 + \alpha_a^{\pm} \exp\left(\beta_a^{\pm} \frac{Q - q_a^{\pm}}{q_a^{\pm}} \right).$$

Here the parameters $\alpha_a^{\pm}$ and $\beta_a^{\pm}$ are fitted to some reference data, and the values $q_a^{\pm}$ are defined in terms of the flow limits $Q_{a\nu}^{\pm}$ of individual pumps,

$$q_a^- = \min \left\{ Q_{a\nu}^- \right\}_{\nu=1}^{N_a}, \quad q_a^+ = \sum_{\nu=1}^{N_a} Q_{a\nu}^+.$$

This model strongly discourages operation in the infeasible ranges $0 < Q_a < q_a^-$ and $q_a^+ < Q_a$ through small values of the efficiency, see Fig. 2.

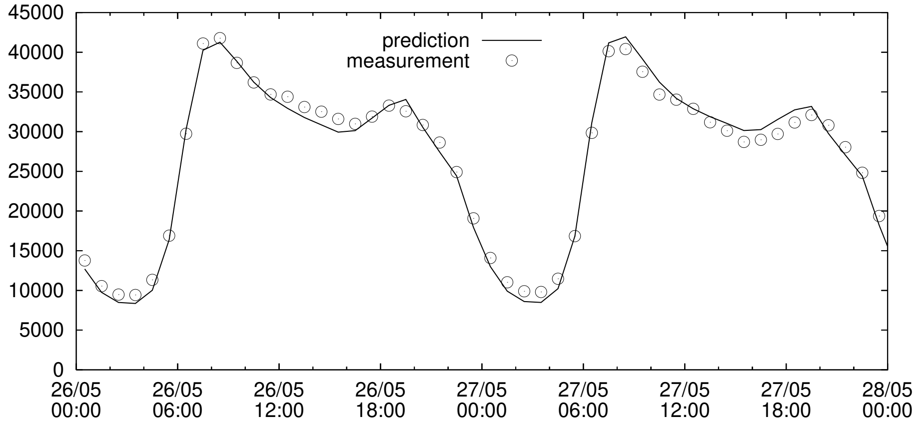

FIGURE 3. Typical profile of network-wide hourly demand in Berlin (m^3)

We consider three categories of typical further constraints differing among certain subsets of the pumps. In raw water pumps, $a \in \mathcal{A}_{\text{pr}}$, additional bounds on the gradient of the flow rate ensure the required quality of the filtering process,

$$c^{\text{grad}}_{at} \triangleq Q_{at} - Q_{a,t-1} \in [\Delta Q^-_{at}, \Delta Q^+_{at}]. \tag{10}$$

At the waterworks outlets, $a \in \mathcal{A}_{\text{po}}$, additional bounds on the total daily discharge may be used to model contractual limits or the amount of available raw water,

$$c^{\text{day}}_{at} \triangleq \Delta t \sum_{t=1}^{T} Q_{at} \in [\Sigma Q^-_{at}, \Sigma Q^+_{at}].$$

In each waterworks or pumping station, $w \in \mathcal{W}$, finally, a bound on the combined power consumption of all raw water pumps $a \in \mathcal{A}_{\text{pr}}(w)$ and pure water pumps $a \in \mathcal{A}_{\text{pp}}(w)$ may reduce costs under graduated electricity tariffs depending on the peak power,

$$c^{\text{pow}}_{wt} \triangleq \sum_{a \in \mathcal{A}_{\text{pr}}(w)} w_{\text{raw},at} Q_{at} + \sum_{a \in \mathcal{A}_{\text{pp}}(w)} \frac{\rho g \Delta H_{at} Q_{at}}{\eta_a(Q_{at})} \le P^+_w.$$

1.9. **Valve Model.** The pressure in a valve $a = ij \in \mathcal{A}_{\text{vl}}$ is decreased by some controlled amount ΔH_{at},

$$c^{\text{diff}}_{at} \triangleq H_{jt} - H_{it} + \Delta H_{at} = 0. \tag{11}$$

To ensure consistency of the pressure decrease with the generally unknown direction of flow, we need a sign condition

$$c^{\text{sign}}_{at} \triangleq \Delta H_{at} Q_{at} \ge 0. \tag{12}$$

The status of a valve may also be prescribed to be permanently closed or open during period t, which instead of (12) leads to respective constraints of the form

$$\Delta H_{at} = 0 \quad \text{or} \quad Q_{at} = 0.$$

1.10. **Demand Model.** Our general model allows individual demand profiles D_{jt} to be specified at all junctions. In practice, the demand forecast often yields predictions of the cumulative demand only, and the local demand at every junction is modeled as a constant fraction of the time-dependent cumulative demand. Such is the current situation in Berlin. An hourly demand profile from late May 2004 is shown in Fig. 3.

TABLE 2. Notation for the cost function.

Symbol	Explanation	Unit
K	Total daily operating cost	€
$k_{\text{el},at}$	Price for electric energy at pump a during period t	€/J
$k_{\text{raw},at}$	Specific price for raw water and treatment materials at pump a	€/m^3
$w_{\text{raw},a}$	Specific work for raw water pumping and treatment at pump a	J/m^3

1.11. **Initial and Terminal Conditions.** Relevant initial values are the tank filling levels and the flow rates of raw water pumps, entering into constraints (2) and (10),

$$H_{j0}, \quad j \in \mathcal{N}_{\text{tk}},$$
$$Q_{a0}, \quad a \in \mathcal{A}_{\text{pr}}.$$

Tightened lower bounds on the tank filling levels prevent undesired finite horizon effects,

$$H_{jT} \geq H_{jT}^{-}, \quad j \in \mathcal{N}_{\text{tk}}. \tag{13}$$

Further initial values will be required for the minimum up and down time constraints developed in Section 3.2, namely the remaining pump flows

$$Q_{a0}, \quad a \in \mathcal{A}_{\text{pp}}.$$

1.12. **Objective Function.** The overall goal is to minimize the variable operating costs,

$$K = \Delta t \sum_{t=1}^{T} (K_{\text{raw},t} + K_{\text{pure},t}), \tag{14}$$

where the respective contributions from raw and pure water production can be written

$$K_{\text{raw},t} = \sum_{a \in \mathcal{A}_{\text{pr}}} (w_{\text{raw},a} k_{\text{el},at} + k_{\text{raw},at}) Q_{at}, \tag{15}$$

$$K_{\text{pure},t} = \sum_{a \in \mathcal{A}_{\text{pp}}} k_{\text{el},at} \frac{\rho g \Delta H_{at} Q_{at}}{\eta_a(Q_{at})}. \tag{16}$$

Thus raw water production causes material and energy costs, both linear in the flow rate, while pure water production causes only energy costs that depend nonlinearly on the flow. The coefficients are listed in Table 2.

1.13. **NLP Formulation.** The decision vector of time-step t consists of node pressures H_{jt}, arc flows Q_{at}, and pressure differences ΔH_{at} at pumps and valves,

$$x_t = \begin{pmatrix} \{H_{jt}\}_{j \in \mathcal{N}} \\ \{Q_{at}\}_{a \in \mathcal{A}} \\ \{\Delta H_{at}\}_{a \in \mathcal{A}_{\text{pu}} \cup \mathcal{A}_{\text{vl}}} \end{pmatrix} \in \mathbf{R}^n, \quad n = |\mathcal{N}| + |\mathcal{A}| + |\mathcal{A}_{\text{pu}} \cup \mathcal{A}_{\text{vl}}|,$$

giving the NLP decision vector

$$x = (x_1, \ldots, x_T) \in \mathbf{R}^N, \quad N = nT.$$

Here we do not make a distinction between state and control variables, and fixed initial values x_0 are not included in x.

The equality constraints in each time-step are comprised of one equation per network element (node or arc),

$$c_t^{\mathcal{E}}(x_{t-1}, x_t) = \begin{pmatrix} \{c_{jt}^{\text{flow}}(x_t)\}_{j\in\mathcal{N}_{\text{jc}}} \\ \{c_{jt}^{\text{head}}(x_t)\}_{j\in\mathcal{N}_{\text{rs}}} \\ \{c_{jt}^{\text{flow}}(x_{t-1}, x_t)\}_{j\in\mathcal{N}_{\text{tk}}} \\ \{c_{at}^{\text{loss}}(x_t)\}_{a\in\mathcal{A}_{\text{pi}}} \\ \{c_{at}^{\text{diff}}(x_t)\}_{a\in\mathcal{A}_{\text{pu}}\cup\mathcal{A}_{\text{vl}}} \end{pmatrix} \in \mathbf{R}^{|\mathcal{N}|+|\mathcal{A}|},$$

yielding

$$c^{\mathcal{E}}(x) = \begin{pmatrix} c_1^{\mathcal{E}}(x_0, x_1) \\ \vdots \\ c_T^{\mathcal{E}}(x_{T-1}, x_T) \end{pmatrix} = 0.$$

The number of variables and constraints per time-step can be reduced by $|\mathcal{N}_{\text{rs}}|$ if the constant reservoir pressures are treated as parameters. In any case, there are $|\mathcal{A}_{\text{pu}}\cup\mathcal{A}_{\text{vl}}|$ degrees of freedom per time-step corresponding to the number of controlled network elements.

The inequality constraints are comprised of upper and lower range constraints and simple bounds on all variables,

$$c^{\mathcal{R}}(x) \in [c^-, c^+], \quad x \in [x^-, x^+],$$

with range constraints

$$c^{\mathcal{R}}(x) = \begin{pmatrix} c_1^{\mathcal{R}}(x) \\ \vdots \\ c_T^{\mathcal{R}}(x) \end{pmatrix}.$$

The components of $c^{\mathcal{R}}$ in each time-step include the nontrivial inequalities from the pumps and valves,

$$c_t^{\mathcal{R}}(x) = \begin{pmatrix} \{c_{at}^{\text{grad}}(x_{t-1}, x_t)\}_{a\in\mathcal{A}_{\text{pr}}} \\ \{c_{wt}^{\text{pow}}(x_t)\}_{w\in\mathcal{W}} \\ \{c_{at}^{\text{day}}(x)\}_{a\in\mathcal{A}_{\text{po}}} \\ \{c_{at}^{\text{sign}}(x_t)\}_{a\in\mathcal{A}_{\text{vl}}} \end{pmatrix} \in \mathbf{R}^{|\mathcal{A}_{\text{pr}}|+|\mathcal{W}|+|\mathcal{A}_{\text{po}}|+|\mathcal{A}_{\text{vl}}|}.$$

Note that the daily discharge limit in waterworks outlets depends on all decision vectors x_t and that the tank flow balances and the gradient constraints in the raw water pumps depend on the current and previous decision vectors x_t, x_{t-1}; all other constraints depend only on the current decision vector x_t.

Finally, the separable objective can be written

$$f(x) = \sum_{t=1}^{T} f_t(x_t) = \sum_{t=1}^{T} \left[f_t^{\text{raw}}(x_t) + f_t^{\text{pure}}(x_t)\right],$$

where f_t^{raw} and f_t^{pure} are given according to (14), (15) and (16) as

$$f_t^{\text{raw}}(x_t) = \sum_{a\in\mathcal{A}_{\text{pr}}} f_{at}^{\text{raw}}(Q_{at}) = \sum_{a\in\mathcal{A}_{\text{pr}}} (w_{\text{raw},a} k_{\text{el},at} + k_{\text{raw},at}) Q_{at}\,\Delta t,$$

$$f_t^{\text{pure}}(x_t) = \sum_{a\in\mathcal{A}_{\text{pp}}} f_{at}^{\text{pure}}(Q_{at}, \Delta H_{at}) = \sum_{a\in\mathcal{A}_{\text{pp}}} k_{\text{el},at} \frac{\rho g \Delta H_{at} Q_{at}}{\eta_a(Q_{at})}\,\Delta t.$$

Thus we obtain a highly structured NLP model in standard form:

$$\operatorname*{Minimize}_{x} \quad f(x) \quad \text{subject to} \quad c^{\mathcal{E}}(x) = 0, \quad c^{\mathcal{I}}(x) \ge 0,$$

where

$$c^{\mathcal{I}}(x) = \begin{pmatrix} c^{\mathcal{R}}(x) - c^{-} \\ c^{+} - c^{\mathcal{R}}(x) \\ x - x^{-} \\ x^{+} - x \end{pmatrix}.$$

2. Convergence Acceleration

One of the primary goals in developing the optimization approach presented here was to achieve acceptable response times for daily planning. Since we are restricted to work with general purpose NLP solvers available under GAMS, exploiting the characteristic NLP structure by special algorithmic developments is not an option. We have to rely on convergence enhancement and other techniques. For convergence acceleration, the most effective measures turned out to be a suitable model formulation and a special initialization strategy for the iterative solution.

2.1. **Model Smoothness.** The objective and constraints in our model are all twice continuously differentiable (C^2), except for the pipe friction loss $\Delta H(Q) = r(Q)\, Q|Q|$. In the piecewise quadratic PKr model ΔH^{PKr}, the second order derivative has respective constant values $-2r^{\text{PKr}}$ and $+2r^{\text{PKr}}$ for $Q < 0$ and $Q > 0$, producing a jump discontinuity at $Q = 0$. Thus ΔH^{PKr} is C^1 only. The more accurate HP-PC model $\Delta H^{\text{HP-PC}}$ is not even continuous at the transition from laminar to turbulent flow [6].

Since the available solvers use derivatives up to first order (MINOS) or second order (CONOPT and SNOPT), numerical difficulties must be expected on a C^1 (or even less smooth) model whenever the flow variables traverse discontinuities between subsequent NLP iterations. This will typically happen during the initial phase of the iterative solution (i.e., far from the optimum, where large steps are taken) whereas it is less likely during the final phase of local convergence.

To avoid such numerical difficulties, we recommend the smoothed PKr model (7) as global approximation of the pipe friction loss,

$$\Delta H_a^{\text{PKrs}}(Q) = r_a^{\text{PKr}} \left(\sqrt{Q^2 + a_a^2} + b_a + \frac{c_a}{\sqrt{Q^2 + d_a^2}} \right) Q.$$

Here the parameters $a_a > 0$ and $d_a > 0$ may be chosen to match a desired slope at $Q = 0$ and to balance the relative contributions of the two square root terms, whereas $b_a > 0$ and $c_a < 0$ depend on the pipe dimensions. They are determined such that, asymptotically for $|Q| \to \infty$, the law of Prandtl–Colebrook is approximated up to second order [6],

$$b_a = 2\delta_a, \quad c_a = (\ln \beta_a + 1)\delta_a^2 - \frac{a_a^2}{2},$$

where

$$\alpha_a = \frac{2.51}{4/(\pi \upsilon d_a)}, \quad \beta_a = \frac{k_a/d_a}{3.71}, \quad \delta_a = \frac{2\alpha_a}{\beta_a \ln 10}.$$

If accuracy requirements are moderate, the PKrs model can easily be simplified by setting $c_a = 0$ or even $b_a = c_a = 0$. This may be appropriate, for instance, to save computational effort during early NLP iterations.

The numerical effect of the smoothing depends heavily on other circumstances. Computational experiments show that, on the test configuration, the smoothing yields significant convergence improvements for CONOPT and SNOPT (the SQP methods) with default initialization heuristics, whereas MINOS (the augmented Lagrangian method) is hardly affected at all. Moreover, SNOPT is slightly faster than MINOS on average. Interestingly, the advantage of the C^2 PKrs model over the C^1 PKr model disappears when we introduce the SLP-based initialization scheme of Section 2.2; now MINOS performs equally well on both formulations, and always better than SNOPT. Another change in the picture occurs when we switch to the much larger main network model. Here the smoothing is beneficial for both solvers, with MINOS still outperforming SNOPT on average. (Apparently, due to rapid convergence within about 20 major iterations, the BFGS updates in SNOPT cannot build up sufficient curvature information to give an advantage.) In practice, we therefore use MINOS on the C^2 model.

2.2. **Initial Estimates.** Computational experiments with artificially perturbed optimal solutions (we added 10% white noise) confirm the expectation that rapid convergence can be achieved when the initial iterate is close to a solution. To exploit this fact, we devised an automatic initialization scheme based on LP approximations of the NLP model. Such approximations are rather crude but quickly solvable with standard LP software (we use CPLEX), so that physically meaningful initial estimates are generated with little effort. Repeating the LP approximation several times yields an initialization scheme of SLP type (sequential linear programming).

The basic idea of SLP approaches in the literature (cf. [7, 13, 22]) is to replace the expensive QP in SQP methods (sequential quadratic programming) by a simpler LP subproblem, obtaining an estimate of the active set at little cost even for very large problems:

$$\begin{aligned} &\text{(17)} && \underset{s}{\text{Minimize}} && g_k^* s \\ &\text{(18)} && \text{subject to} && J_k^{\mathcal{E}} s + c_k^{\mathcal{E}} = 0, \\ &\text{(19)} && && J_k^{\mathcal{I}} s + c_k^{\mathcal{I}} \geq 0, \\ &\text{(20)} && && \|s\|_\infty \leq \delta. \end{aligned}$$

Here the trust region constraint is introduced to ensure global convergence and to prevent unboundedness, and the LP data are generated as standard linearization of the problem functions. Thus g_k is the gradient of the objective, $c_k^{\mathcal{E}}, c_k^{\mathcal{I}}$ are the respective residuals of equality and inequality constraints, and $J_k^{\mathcal{E}}, J_k^{\mathcal{I}}$ are the associated Jacobians:

$$\begin{aligned} g_k &= \nabla f(x^k), & c_k^{\mathcal{E}} &= c^{\mathcal{E}}(x^k), & J_k^{\mathcal{E}} &= \nabla c^{\mathcal{E}}(x^k)^*, \\ & & c_k^{\mathcal{I}} &= c^{\mathcal{I}}(x^k), & J_k^{\mathcal{I}} &= \nabla c^{\mathcal{I}}(x^k)^*. \end{aligned}$$

The LP solution s^k serves to determine a working set of currently active constraints, based on which a better second order step is usually calculated. Only if this fails is s^k taken as step direction for the SLP.

Since the LP (17)–(20) may be infeasible even if the NLP is feasible, it is appropriate to minimize the ℓ_1 penalty function instead, subject only to the trust region constraint,

$$\text{(21)} \qquad \underset{s}{\text{Minimize}} \quad \ell_1(s,\rho) \quad \text{subject to} \quad \|s\|_\infty \leq \delta,$$

where

$$\begin{aligned} \ell_1(s,\rho) &\triangleq g_k^* s + \rho \|J_k^{\mathcal{E}} s + c_k^{\mathcal{E}}\|_1 + \rho \|\min(J_k^{\mathcal{I}} s + c_k^{\mathcal{I}}, 0)\|_1 \\ &= g_k^* s + \rho \sum_{i\in\mathcal{E}} |J_k^i s + c_k^i| + \rho \sum_{i\in\mathcal{I}} |\min(J_k^i s + c_k^i, 0)|. \end{aligned}$$

For the numerical solution, the nonsmooth ℓ_1 problem is finally converted to LP form by standard techniques (see, e.g., [8]), yielding the problem

$$\begin{aligned} &\text{(22)} && \underset{s, s_+^{\mathcal{E}}, s_-^{\mathcal{E}}, s_-^{\mathcal{I}}}{\text{Minimize}} && g_k^* s + \rho e^*(s_+^{\mathcal{E}} + s_-^{\mathcal{E}}) + \rho e^* s_-^{\mathcal{I}} \\ &\text{(23)} && \text{subject to} && J_k^{\mathcal{E}} s + c_k^{\mathcal{E}} - s_+^{\mathcal{E}} + s_-^{\mathcal{E}} = 0, \qquad s_+^{\mathcal{E}}, s_-^{\mathcal{E}} \geq 0, \\ &\text{(24)} && && J_k^{\mathcal{I}} s + c_k^{\mathcal{I}} \phantom{- s_+^{\mathcal{E}}} + s_-^{\mathcal{I}} \geq 0, \qquad s_-^{\mathcal{I}} \geq 0, \\ &\text{(25)} && && \|s\|_\infty \leq \delta. \end{aligned}$$

Here the nonnegative slack variables $s_+^{\mathcal{E}}, s_-^{\mathcal{E}}, s_-^{\mathcal{I}}$ represent positive and negative violations of equality and inequality constraints, respectively, and e denotes the vector of ones in appropriate dimensions. It is easily seen that the modified LP (22)–(25) is always feasible. Moreover, if the penalty parameter ρ is sufficiently large, the slacks of an optimal solution vanish if and only if the original LP is feasible, in which case both problems yield the same optimal value for the step s.

Our problem-specific scheme deviates from the general approach in several respects:

2.2.1. *Linearization.* Observe first that nonlinearities arise only in the pressure loss equations c^{loss}_{at}, in the valve constraints c^{sign}_{at}, and in the objective. These nonlinearities are handled as follows.

(1) The PKr friction model is used, and the absolute volumetric flow rates $|Q_{at}|$ are replaced with constant parameters $\bar{Q}_{at} > 0$. The pressure loss (4) then reads

$$H_{jt} - H_{it} - r^{\text{PKr}}_a \bar{Q}_{at} Q_{at} = 0.$$

For the parameter $\bar{Q}_{at}$ we use a heuristic initial estimate defined as a constant multiple of the pipe diameter, $\bar{Q}^0_{at} = \bar{c} d_a$. (In practice, a reasonable value may be available from optimal solutions of the past.) In iteration k, the flow components Q^k_{at} of the LP solution are then used to update the parameter values,

$$\bar{Q}^{k+1}_{at} = \alpha \bar{Q}^k_{at} + (1-\alpha)|Q^k_{at}|,$$

where we choose $\alpha = 0.6$ as weighting factor in the convex combination.

(2) Assuming temporarily that the direction of flow is known in all valves, the sign condition is replaced by two simple bounds,

$$Q_{at} \geq 0, \quad \Delta H_{at} \geq 0 \quad \text{or} \quad Q_{at} \leq 0, \quad \Delta H_{at} \leq 0.$$

The dual LP solution then yields directional information for the next LP iteration: if any of the simplified constraints are binding, the sign of both constraints can be switched on the assumption that the chosen direction of flow was not optimal.

(3) The nonlinear term $\Delta H_{at} Q_{at}/\eta(Q_{at})$ in the pump efficiency model entering the cost function is handled as follows. The pressure difference ΔH_{at} is replaced with a constant parameter that is iteratively updated like $\bar{Q}_{at}$. The quotient $Q_{at}/\eta(Q_{at})$ is approximated by a strictly increasing convex piecewise linear function of Q_{at} that consists of three segments and starts at the origin.

Thus our LP is a local *approximation* of the NLP yielding the iterate x^k, rather than a local *linearization* yielding a step direction s^k at the given iterate. Moreover, we do not use any second order information.

2.2.2. *Trust Region.* We do not impose a trust region constraint in addition to the bounds on all variables, since we are not interested in global or local convergence properties of the SLP method but only in getting a cheap initial estimate for the NLP iteration. In practical computations we usually perform three SLP-type steps before switching to the fully nonlinear model. According to our experience (based on a large number of numerical experiments), this yields the best performance for the network of Berliner Wasserbetriebe.

2.2.3. *Penalty.* The ℓ_1 penalty approach ensuring feasibility is only applied to selected constraints, namely to the pressure limits at pressure measurement points and at the outlets of waterworks and pumping stations. These constraints are relaxed in the LP as well as in the NLP model.

A relaxation of *all* inequality constraints is applied in a second version of our operative planning model. This version is used after physical modifications of the network to detect potential infeasibilities caused by errors in the mathematical formulation or input data.

2.2.4. *Remarks.* A pure SLP approach has also been tested. The performance was generally inferior to the combined LP/NLP approach; often the iteration did not even converge.

Finally we tried to catch the combinatorial aspects of the problem explicitly during the SLP initialization procedure, by replacing the LP approximations with similar mixed-integer linear programs (MIP). Even with SOS Type 2 formulations of the piece-wise linear approximation of the pressure loss equations (cf. [30, 35, 37]), solving the MIP subproblems took so long that no benefit could be achieved.

2.3. **Further Attempts.** Several additional convergence acceleration methods have been tested, but none of them led to significant improvements. We give some brief comments on these attempts.

2.3.1. *Scaling.* We have compared four scaling strategies: manual scaling and the three automatic scaling options that GAMS offers,

(0) ”no” scaling (all scale factors are equal to one);
(1) automatic scaling of linear variables and constraints (the default);
(2) automatic scaling of all variables and constraints.

As expected, manual scaling led to the best results after some empirical adjustments of the scaling factors. The default scaling performed almost equally well whereas the performance with ”no” scaling or with automatic scaling of all variables and constraints was rather poor. Since the manual scaling usually requires some parameter tuning to adjust for the input data (demand profile, initial state of network, availability of technical equipment), the default scaling was retained as most reasonable choice for routine operation.

2.3.2. *Spatial Decomposition.* The topographical situation of Berlin suggests a network decomposition into three natural pressure zones: the southern uptown (Teltowhochfläche), the downtown valley of river Spree (Urstromtal), and the northeastern uptown (Barnimhochfläche). After the SLP initialization, we tried to improve the initial estimates through local NLP solutions for each of the three pressure zones, with prescribed pressure and flow values at their boundaries taken from the last LP solution. As it turned out, no reduction in the total computation time could be achieved. When no deviations or small deviations from the boundary values were permitted, the local NLP subproblems were often infeasible or convergence was slow. When larger deviations were permitted, convergence was slow on the recombined network. In any case, the total computation time exceeded the computation time on the undecomposed model.

2.3.3. *Initialization from Database.* Berliner Wasserbetriebe maintains a database of actual network operation over several years. This database records the hourly profiles of all relevant quantities, such as the raw water and pure water production, outlet pressures, valve positions, tank filling levels, etc. It does not include flow and pressure profiles for the entire network, however. To generate a good initial estimate for the current planning period from the recorded data of a similar previous day, we calculated the missing data from an (overdetermined) least-squares problem. Again it turned out that no savings in total computation time could be achieved; sometimes the initialization procedure just described took already longer than solving the full operative planning problem from scratch.

3. COMBINATORIAL ISSUES

Combinatorial aspects addressed here include the direction of flow across valves and the switching of speed-controlled pumps. Further aspects that may occur in water networks include the switching of fixed-speed pumps [6] and the choice among alternative waterworks outlets. The latter issues involve purely integral decisions that can to date not be treated satisfactorily in an NLP setting, although nonlinear programs with certain combinatorial structures (complementarity constraints and equilibrium constraints) have recently been studied and successfully solved by suitably extended NLP methods [2, 23, 42, 46, 48].

3.1. **Flow Direction across Valves.** The valve sign condition (12) has some undesirable properties at the origin, where the gradient vanishes and no constraint qualification holds. This reflects the geometry of the feasible set: consisting of two opposite closed quadrants, it has disconnected interior and becomes itself disconnected if the origin is removed. One might think that the direction of flow should therefore be introduced as a binary decision variable, but a detailed analysis reveals that no numerical difficulties are to be expected as long as the gradient of the Lagrangian (projected into the relevant subspace) does not vanish at the origin. Since the latter condition is generically satisfied, we do not need to reformulate the model.

3.2. **Pump Switching.** Computational experience shows that optimal solutions frequently exhibit undesirable pump switching at the waterworks outlets:

- short-term activation of a pump for just one or two periods;
- short-term deactivation of a pump for just one or two periods;
- alternating discharge: a certain flow rate is produced by two or more waterworks outlets alternating in time.

Operating schedules like these reduce the pump lifetime and require increased activity of the operators.

Specifying minimum up and down times is straightforward in a mixed-integer model. Let $Y_{at} \in \{0, 1\}$ designate the activity status of pump $a \in \mathcal{A}_{pp}$; cf. [6]. Then the following linear inequality constraints, specified at $t = 0, \dots, T - K$, freeze the status for at least K periods after a switch:

$$K(Y_{a,t+1} - Y_{at}) \leq Y_{a,t+1} + \cdots + Y_{a,t+K} \leq 2K(Y_{a,t+1} - Y_{at}) + K.$$

In a pure NLP setting it is unclear how to obtain a similar effect.

To avoid unnecessary pump switching, several mathematical and heuristic techniques have therefore been devised and tested. They can be categorized into three major groups:

(1) penalty approach;
(2) linear, piece-wise linear, and nonlinear constraints (C^0 or C^2);
(3) heuristics.

In summary, most of the techniques proved either little successful or rather slow. However, we did find computationally cheap smooth constraints (group 2) that suppress the undesired behavior, either with certainty (pump activation) or with high reliability (deactivation).

3.2.1. *Avoiding Short-Term Pump Activation.* As it turns out, activation of pumps for one or two periods can be prevented with certainty by suitable *linear* inter-temporal constraints. Formally, we wish to inhibit flow sequences of the types

(1) $(Q_t, Q_{t+1}, Q_{t+2}) = (0, Q_{t+1}, 0)$ with $Q_{t+1} > 0$, or
(2) $(Q_t, Q_{t+1}, Q_{t+2}, Q_{t+3}) = (0, Q_{t+1}, Q_{t+2}, 0)$ with $Q_{t+1}, Q_{t+2} > 0$.

The basic idea is to prevent excessive concavity of the piece-wise constant flow rate profiles (1) and (2) by placing appropriate lower bounds on their discrete curvatures. In case (1), such a condition may be formulated as

$$Q_t - 2Q_{t+1} + Q_{t+2} \geq -c_1(Q_t + Q_{t+1} + Q_{t+2}), \quad t = 0, \dots, T - 2, \tag{26}$$

where $c_1 > 0$ is a constant parameter. The flow-dependent right-hand side allows for larger values of the concavity with increasing total flow. A suitable range for the value of the parameter c_1 is determined as follows. In the case of interest, $Q_t = Q_{t+2} = 0$, condition (26) yields

$$-2Q_{t+1} \geq -c_1 Q_{t+1},$$

so that one must choose $c_1 < 2$ to force Q_{t+1} to zero, as desired. On the other hand, we do not wish to rule out otherwise feasible pump operation: if c_1 is chosen unreasonably small, then condition (26) will become too restrictive. This is immediately seen in the equivalent form

$$Q_{t+1} \leq \frac{1+c_1}{2-c_1}(Q_t + Q_{t+2}), \tag{27}$$

which implies, for instance, $Q_{t+1} \leq \frac{1}{2}(Q_t + Q_{t+2})$ if $c_1 = 0$, and $Q_{t+1} = 0$ for all t if $c_1 \leq -1$. To find a lower bound on c_1, we rewrite (26) as

$$(1+c_1)(Q_t + Q_{t+2}) - (2-c_1)Q_{t+1} \geq 0$$

and determine the minimum of the left-hand expression over the nontrivial feasible flow sequences, $\{Q_t, Q_{t+1}, Q_{t+2} \in \{0\} \cup [Q^-, Q^+] \colon Q_t \neq 0 \text{ or } Q_{t+2} \neq 0\}$. This yields

$$(1+c_1)Q^- - (2-c_1)Q^+ \geq 0,$$

which is realized by the extremal flow sequences

$$(0, Q^+, Q^-) \quad \text{and} \quad (Q^-, Q^+, 0).$$

Letting

$$\alpha = \frac{Q^+}{Q^-} > 1 \quad \text{and} \quad \beta_1 = \frac{2\alpha - 1}{\alpha + 1} \in (\tfrac{1}{2}, 2),$$

the minimal left-hand expression above is finally seen to be nonnegative if and only if

$$c_1 \in [\beta_1, 2) \quad \text{where} \quad [\beta_1, 2) \neq \emptyset.$$

Similar reasoning for the two-period case (2) yields the restriction

$$Q_t - Q_{t+1} - Q_{t+2} + Q_{t+3} \geq -c_2(Q_t + Q_{t+1} + Q_{t+2} + Q_{t+3}), \quad t = 0, \dots, T-3.$$

Here one must require $c_2 < 1$ to prevent undesired pump activation, and a lower bound β_2 is obtained with the reformulation

$$(1+c_2)(Q_t + Q_{t+3}) - (1-c_2)(Q_{t+1} + Q_{t+2}) \geq 0.$$

Minimizing the left-hand expression yields extremal flow sequences

$$(0, Q^+, Q^+, Q^-) \quad \text{and} \quad (Q^-, Q^+, Q^+, 0),$$

and the condition

$$(1+c_2)Q^- - (1-c_2)(2Q^+) \geq 0.$$

Thus we finally get

$$c_2 \in [\beta_2, 1) \quad \text{where} \quad \beta_2 = \frac{2\alpha - 1}{2\alpha + 1} \in (\tfrac{1}{3}, 1), \quad \text{and} \quad [\beta_2, 1) \neq \emptyset.$$

In summary, the following linear inequalities prevent undesired pump activation for one or two periods with certainty without being too restrictive:

$$\begin{aligned} (c_1+1)Q_t + (c_1-2)Q_{t+1} + (c_1+1)Q_{t+2} &\geq 0, \quad c_1 \in (\tfrac{1}{2}, 2), \\ (c_2+1)Q_t + (c_2-1)Q_{t+1} + (c_2-1)Q_{t+2} + (c_2+1)Q_{t+3} &\geq 0, \quad c_2 \in (\tfrac{1}{3}, 1). \end{aligned}$$

These restrictions are specified for each pump in almost all time-steps, yielding the large number of $O(|\mathcal{A}_{\mathrm{pu}}|T)$ extra conditions. Despite this, no adverse effect on the computation time was observed on our problem instances.

3.2.2. *Avoiding Short-Term Deactivation of Pumps.* Linear restrictions in the spirit of (26) are unfortunately not useful in avoiding short-term deactivation. To see this, assume that $(Q_t, 0, 0)$ and $(0, 0, Q_{t+2})$ are feasible and all feasible sequences satisfy the constraint

$$aQ_t + bQ_{t+1} + cQ_{t+2} + d \geq 0.$$

Now, the sum $(Q_t, 0, Q_{t+2})$ is forbidden but satisfies the same constraint. The asymmetry arises from the fact that during activation the initial and final flow rates are both exactly known and identical, $Q_t = Q_{t+2} = 0$, whereas only $Q_{t+1} = 0$ is known during deactivation. In general, Q_t and Q_{t+2} are neither known nor identical in the latter case.

To inhibit short-term deactivation, we suggest to specify a certain fraction of the minimum of the enclosing values as lower bound on the intermediate flow rate, thus arriving at the piecewise linear constraint

$$Q_{t+1} \geq c \min(Q_t, Q_{t+2}), \quad t = 0, \ldots, T-2,$$

with an appropriate parameter range of $c \in (0, 1]$. This formulation does the job but slows down convergence dramatically, which is not surprising since the minimum function is not differentiable but only continuous (C^0). Using the standard reformulation in terms of the absolute value function,

$$Q_{t+1} \geq \frac{c}{2}(Q_t + Q_{t+2} - |Q_t - Q_{t+2}|),$$

one can now apply the smoothing $|x| = \sqrt{x^2} \approx \sqrt{x^2 + \alpha^2}$ to obtain the C^2 formulation

$$Q_{t+1} \geq \frac{c}{2}\Big(Q_t + Q_{t+2} - \sqrt{(Q_t - Q_{t+2})^2 + \alpha^2}\Big).$$

Finally we redefine c to arrive at the nonlinear inequality

$$Q_{t+1} - c\Big(Q_t + Q_{t+2} - \sqrt{(Q_t - Q_{t+2})^2 + \alpha^2}\Big) \geq 0, \quad c \in (0, \tfrac{1}{2}]. \tag{28}$$

The two-period version consists of two similar inequalities with identical parameters,

$$Q_{t+i} \geq c \min(Q_t, Q_{t+3}), \quad i = 1, 2, \quad t = 0, \ldots, T-3,$$

yielding the smooth reformulation

$$Q_{t+i} - c\Big(Q_t + Q_{t+3} - \sqrt{(Q_t - Q_{t+3})^2 + \alpha^2}\Big) \geq 0, \quad c \in (0, \tfrac{1}{2}], \quad i = 1, 2. \tag{29}$$

Note that the constraints (28), (29) are always compatible with the flow bounds and flow gradient bounds.

4. Model Reduction

Due to excessive computation times with the main network (even in the case of rapid convergence) the need for a systematic reduction of the size of the network graph arose. Such a reduction is performed as preprocessing before the optimization; it is based solely on static network data, so that a single reduced graph is used over the entire horizon.

The reduction leads to simplified models for the pipe friction loss, where we calculate the leading coefficient from the PKr model to ensure asymptotically correct friction loss for large flow values $|Q|$. Appropriate smoothing is then introduced for small flow values.

4.1. **Parallel Pipes.** It is not uncommon for municipal water networks to contain pairs of nodes that are connected by several "parallel" pipes. In the network model, such pipe ensembles can be replaced by a single pipe (see Fig. 4), which is hydraulically equivalent if the loss coefficients r_v are flow-independent (PKr model). Consider a collection of n parallel pipes with total flow rate

$$Q = Q_1 + \cdots + Q_n. \tag{30}$$

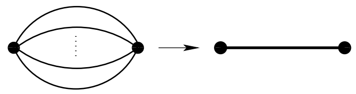

FIGURE 4. Collapsing parallel pipes

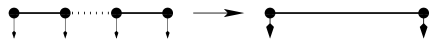

FIGURE 5. Collapsing pipe sequences

Then all the flows Q and Q_ν have the same direction and a common pressure difference,

$$\Delta H = rQ|Q| = r_\nu Q_\nu |Q_\nu|, \quad \nu = 1, \dots, n. \tag{31}$$

The fictitious loss coefficient r of the hydraulically equivalent pipe is readily calculated from (30) and (31). Assuming positive flows with no loss of generality, one obtains

$$\sqrt{\frac{\Delta H}{r}} = Q = \sum_{\nu=1}^{n} Q_\nu = \sum_{\nu=1}^{n} \sqrt{\frac{\Delta H}{r_\nu}},$$

and hence

$$\frac{1}{\sqrt{r}} = \sum_{\nu=1}^{n} \frac{1}{\sqrt{r_\nu}} \iff r = \left(\sum_{\nu=1}^{n} \frac{1}{\sqrt{r_\nu}} \right)^{-2}.$$

Conversely, with (31) the individual flows Q_ν are recovered from the total flow as

$$Q_\nu = \sqrt{\frac{r}{r_\nu}} Q.$$

This is similar to parallel resistors in an electric circuit, except that the flow dependence here is quadratic rather than linear.

To derive the parameters of the smooth approximation (7), the replacement pipe also needs fictitious geometric dimensions. We define the length as the average length of the original pipes, and the diameter such that the total pipe volumes agree,

$$L = \frac{1}{n} \sum_{\nu=1}^{n} L_\nu, \quad d = \sqrt{\frac{1}{L} \sum_{\nu=1}^{n} L_\nu d_\nu^2}.$$

The roughness is finally chosen such that r is consistent with all dimensions according to (5) and (6),

$$r = \frac{8L}{\pi^2 g d^5} \left(2 \log \frac{k/d}{3.71} \right)^{-2},$$

yielding

$$k = 3.71 d \times 10^{\sqrt{2L/(\pi^2 g d^5 r)}}.$$

From these values we readily obtain the required parameters b, c for the PKrs model.

4.2. **Pipe Sequences.** A sequence of n pipes traversing junction nodes $0, \dots, n$ can be collapsed if no other arcs are connected to the interior nodes $1, \dots, n-1$. In this case the interior nodes are eliminated, their demands D_ν are distributed over the two boundary nodes, and the n pipes are replaced by a fictitious single pipe; see Fig. 5.

4.2.1. *Zero Interior Demands.* In the case of vanishing demands, pipes $1, \dots, n$ have identical flow rates, $Q_\nu = Q$, and a hydraulically equivalent model is obtained if and only if the loss coefficient r of the fictitious pipe is defined as the sum of the individual loss coefficients,

$$H_0 - H_n = \sum_{\nu=1}^{n} H_{\nu-1} - H_\nu = \sum_{\nu=1}^{n} r_\nu Q_\nu |Q_\nu| = \sum_{\nu=1}^{n} r_\nu Q|Q| = r\, Q|Q|.$$

This is similar to serial resistors in an electric circuit, and it does not matter whether the coefficients r_ν are assumed to be flow-independent or not.

4.2.2. *Nonzero Interior Demands.* For arbitrary consumption demands it is impossible to construct a hydraulically equivalent reduced model. This is because of three reasons:

(1) the symmetry with respect to the direction of flow is broken in general: inflows of identical magnitudes at nodes 0 and n yield different absolute pressure differences;
(2) the inflow may enter from *both* sides, adding up to the total interior demand;
(3) the pressure difference does not depend quadratically on any linear combination of the flow rates Q_ν, even with quadratic segment losses $r_\nu Q_\nu |Q_\nu|$ (PKr model).

As it turns out, the best fictitious replacement pipe in this case is obtained as follows. With the notation $r_{k:l} \triangleq \sum_{\nu=k}^{l} r_\nu$, let $r = r_{1:n}$ (as above), let $L = L_{1:n}$, and split each interior demand D_ν into fictitious demands $(r_{\nu+1:n}/r)D_\nu$ at node 0 and $(r_{1:\nu}/r)D_\nu$ at node n, according to the relation of friction losses to each endpoint:

$$D_0^{\text{int}} \triangleq \sum_{\nu=1}^{n-1} \frac{r_{\nu+1:n}}{r} D_\nu, \quad D_n^{\text{int}} \triangleq \sum_{\nu=1}^{n-1} \frac{r_{1:\nu}}{r} D_\nu. \tag{32}$$

The actual inflow from node 0 and outflow to node n, Q_1 and Q_n, are thus replaced with a common fictitious flow value, $Q_1 - D_0^{\text{int}} = Q_n + D_n^{\text{int}}$.

As with parallel pipes (see Section 4.1), the diameter d and roughness k of the fictitious pipe are determined such that its loss coefficient r is consistent with the PKr model.

We will now see that one can do better than with such a single pipe replacement model. To investigate this in detail, consider the exact pressure loss in the pipe sequence according to the quadratic PKr model. Since the flow rates in successive pipes are related by

$$Q_{\nu+1} = Q_\nu - D_\nu, \quad \nu = 1, \dots, n-1,$$

we get inductively

$$Q_\nu = Q_1 - \bar{D}_\nu, \quad \nu = 1, \dots, n,$$

where Q_1 is the inflow from node 0 and $\bar{D}_\nu$ denotes the cumulative interior demand up to and including node $\nu - 1$,

$$\bar{D}_\nu = D_{1:\nu-1}, \quad \nu = 1, \dots, n.$$

(Note that $\bar{D}_1 = 0$, giving total interior demand $\bar{D}_n = D_1 + \dots + D_{n-1}$.) Thus we obtain

$$H_0 - H_n = \sum_{\nu=1}^{n} r_\nu Q_\nu |Q_\nu| = \sum_{\nu=1}^{n} r_\nu (Q_1 - \bar{D}_\nu)|Q_1 - \bar{D}_\nu|.$$

Left-Sided Inflow. Consider first the case where $Q_1 \geq \bar{D}_n$ (that is, all flow directions in the pipe sequence are positive) and observe that the coefficients r_ν/r formally satisfy the properties of a probability distribution. Defining the spatial flow distribution vectors $Q = (Q_1, \dots, Q_n)$ and similarly $\bar{D} = (\bar{D}_1, \dots, \bar{D}_n)$ etc., one obtains

$$\begin{aligned} H_0 - H_n &= r \sum_{\nu=1}^{n} \frac{r_\nu}{r} Q_\nu^2 = r\mathbf{E}(Q^2) \\ &= r\left[\mathbf{E}(Q)^2 + \left(\mathbf{E}(Q^2) - \mathbf{E}(Q)^2\right)\right] = r\mathbf{E}(Q)^2 + r\mathrm{Var}(Q). \end{aligned} \tag{33}$$

Here the first term can be interpreted as the pressure loss of a weighted *average* flow rate with respect to the "probabilities" r_ν/r,

$$\sum_{\nu=1}^{n} \frac{r_\nu}{r} Q_\nu = \mathbf{E}(Q) = \mathbf{E}(Q_1 - \bar{D}) = Q_1 - \mathbf{E}(\bar{D}).$$

The second term can be interpreted as an additional pressure loss due to the *variance* of the individual flow rates, which equals the flow-independent variance of the *accumulated* demands,

$$\mathbf{E}(Q^2) - \mathbf{E}(Q)^2 = \mathrm{Var}(Q) = \mathrm{Var}(Q_1 - \bar{D}) = \mathrm{Var}(\bar{D}).$$

Since $\bar{D}_1 = 0$, this variance vanishes if and only if *all* interior demands vanish.

Right-Sided Inflow. Consider next the situation for $Q_1 \le 0$, which is similar to $Q_1 \ge \bar{D}_n$ except that the flow now goes in the opposite direction, and we have a pressure loss from node n to node 0,

$$H_0 - H_n = -r\mathbf{E}(Q)^2 - r\mathrm{Var}(Q) = -r\mathbf{E}(Q)^2 - r\mathrm{Var}(\bar{D}).$$

With the demand redistribution defined in (32), the fictitious pipe's flow rate is $\mathbf{E}(Q)$,

$$Q_1 - D_0^{\text{int}} = Q_1 - \sum_{0<\nu<\mu\le n} \frac{r_\mu}{r} D_\nu = Q_1 - \mathbf{E}(\bar{D}) = \mathbf{E}(Q),$$

thus giving precisely the first term of the pressure loss (33) according to the PKr model. The constant variance term, however, cannot be obtained in this pipe model—a *qualitative* defect of the single pipe replacement (reason 3).

By symmetry, the relevant quantities above can also be expressed in terms of Q_n rather than Q_1. Defining

$$\underline{D}_\nu = D_{\nu:n-1}, \quad \nu = 1, \dots, n,$$

so that $Q_\nu = Q_n + \underline{D}_\nu$ with $\underline{D}_n = 0$ and $\underline{D}_1 = \bar{D}_n$, this yields alternative representations for the actual in- and outflow,

$$\begin{aligned} Q_1 &= Q_1 - \bar{D}_1 = Q_n + \underline{D}_1, \\ Q_1 - \bar{D}_n &= Q_n + \underline{D}_n = Q_n, \end{aligned}$$

and for the (identical) fictitious in- and outflow,

$$Q_1 - D_0^{\text{int}} = Q_1 - \mathbf{E}(\bar{D}) = \mathbf{E}(Q) = Q_n + \mathbf{E}(\underline{D}) = Q_n + D_n^{\text{int}}.$$

Two-Sided Inflow. A second, more serious qualitative defect arises in the situation where $Q_1 \in (0, \bar{D}_n)$, or $-\mathbf{E}(\underline{D}) < \mathbf{E}(Q) < \mathbf{E}(\bar{D})$: then we have inflows from both sides, and the total pressure difference $H_0 - H_n$ depends on the location where the inflows meet in the pipe sequence. This location has minimal pressure within the sequence and occurs either at a unique node whose inflows are both smaller than the local demand, or possibly at a unique pair of nodes whose (one-sided) inflows equal the respective demands, yielding stagnant flow in between. Clearly, this situation cannot be modeled by a single replacement pipe with just one flow direction (reason 2). Without simplifications, the PKr friction model yields a piecewise quadratic dependence where the curvature has jump discontinuities at $Q_1 = \bar{D}_\nu$ (or $Q_n = \underline{D}_\nu$), $\nu = 1, \dots, n$.

Denoting the fictitious flow $\mathbf{E}(Q)$ as Q and the values $-\mathbf{E}(\bar{D}), +\mathbf{E}(\underline{D})$ as D^-, D^+, respectively, we suggest to use a global smoothing for the entire sequence by approximating the pressure difference for $Q \in (D^-, D^+)$ with the unique polynomial of degree five having C^2 junctions with the outer pieces at $Q = D^-$ and $Q = D^+$:

$$\phi(Q) = \sum_{k=0}^{5} c_k Q^k,$$

where the coefficients c_k are obtained from a linear equation system representing the matching conditions.

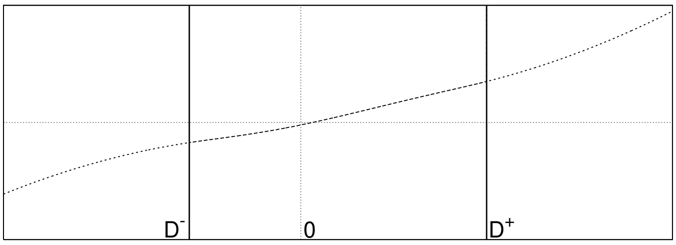

FIGURE 6. Three-piece C^2 model of pressure loss in a pipe sequence

FIGURE 7. Collapsing short pipes and subnetworks

The resulting replacement model ("generalized pipe") has three benefits: the constant variance term is included, inflows from both sides are suitably modeled, and all discontinuities disappear. Letting $V = \mathrm{Var}(\overline{D}) = \mathrm{Var}(\underline{D})$, one thus gets a global C^2 representation consisting of three pieces; see Fig. 6:

$$H_0 - H_n = \Delta H(Q) = \begin{cases} -rQ^2 - rV, & Q \le D^-, \\ r\phi(Q), & Q \in (D^-, D^+), \\ +rQ^2 + rV, & Q \ge D^+. \end{cases}$$

4.3. **Short Pipes.** The pressure loss along a short pipe is often negligible so that the pipe can be collapsed into a single node; see Fig. 7. Such collapsing may even be possible for entire subnetworks (consisting of junctions and sufficiently short pipes only), which is typical for residential or industrial areas.

The following algorithm is used for collapsing subnetworks.

(0) Input: a subset of pipes that must not be removed from the graph, $\mathcal{A}_0 \subset \mathcal{A}_{\text{pi}}$, and the maximal length of a "short" pipe, $L_{\max}$.
(1) Determine the set of short pipes eligible for removal,
$$\mathcal{A}_{\text{short}} = \{a \in \mathcal{A}_{\text{pi}} \setminus \mathcal{A}_0 \colon L_a \le L_{\max}\}.$$
(2) Determine the network subgraph induced by $\mathcal{A}_{\text{short}}$, with connected components $G_l = (\mathcal{N}_l, \mathcal{A}_l)$.
(3) Collapse each connected component G_l to a single junction l having demand D_l:
$$D_l = \sum_{j \in \mathcal{N}_l} D_j.$$

For the network of Berliner Wasserbetriebe, the maximal length of a "short" pipe was empirically set to 500 m after some experiments, since this value gave the best compromise of model accuracy and computation time. The reduced main network then has 413 nodes and 608 links. With increasing computing power, the threshold length may be gradually decreased in the future.

5. RESULTS

We consider the municipal drinking water network of Berliner Wasserbetriebe, which has nine waterworks and eight additional pumping stations, five of which are equipped with tanks. The total length of all pipes is 7800 km. There are 256000 household connections, serving a yearly consumption demand over 200 million m^3 with daily demands ranging between roughly half a million and one million m^3.

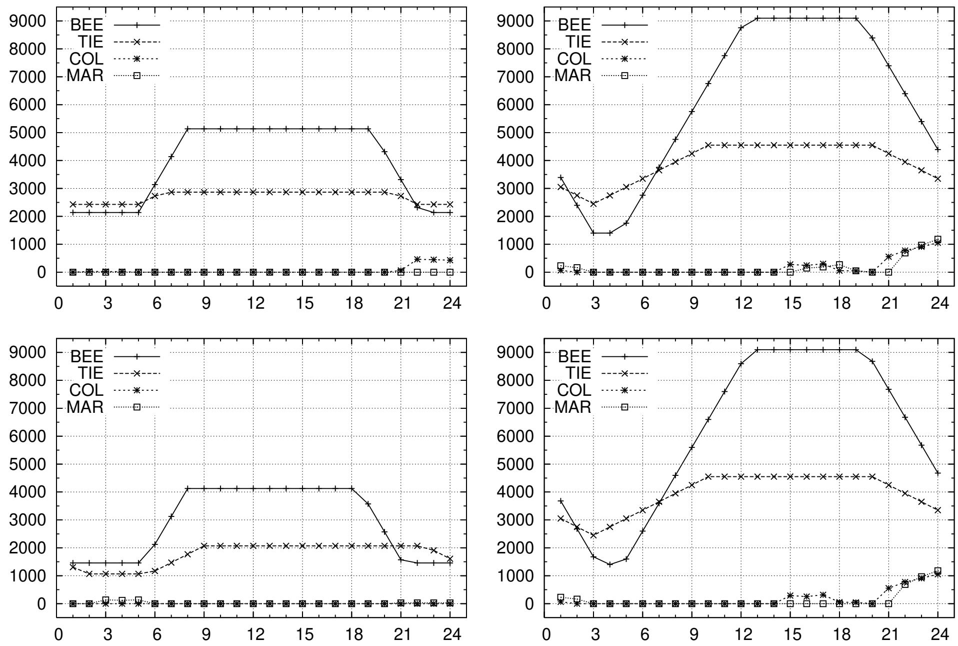

FIGURE 8. Optimal raw water production at BEE and TIE, and tank inflows at COL and MAR (m^3/h). Scenarios 1 (top left), 2 (top right), 3 (bottom left), and 4 (bottom right).

In the waterworks, raw water is extracted via groundwater wells from reservoirs. After treatment, the pure water is stored in tanks and then pumped into the pressurized distribution network. Control actions to be planned include raw water pumping, pure water pumping, filling and emptying the tanks, and setting the control valves.

To investigate how optimal solutions change with the operating conditions, we consider four scenarios with different combinations of

- the demand: normal and high;
- electricity prices: constant and variable;
- groundwater extraction fees: current and previous.

The normal daily demand is $585000\,m^3$, the fictitious high demand is one million m^3.

Electricity prices differ between the providers in Berlin and in the federal state of Brandenburg where the waterworks Stolpe is located. In the scenario with variable electricity prices, a reduction of about 13% has been applied at the waterworks Stolpe during nighttime (18:00-08:00).

The groundwater extraction fees (GEG, *Grundwasserentnahmeentgelt* in German) also differ between the waterworks of Berlin and Brandenburg. They are about six times higher in Berlin compared to the fees in the federal state of Brandenburg. Within Berlin, the current groundwater extraction fees are identical all over the city whereas previous fees were reduced at the waterworks Spandau and Tegel.

In what follows, every figure compares for some quantity of interest the time histories of the following four scenarios:

(1) fixed electricity price, current GEG, normal demand (top left, reference);
(2) fixed electricity price, current GEG, high demand (top right);
(3) fixed electricity price, previous GEG, normal demand (bottom left);
(4) variable electricity price, current GEG, high demand (bottom right).

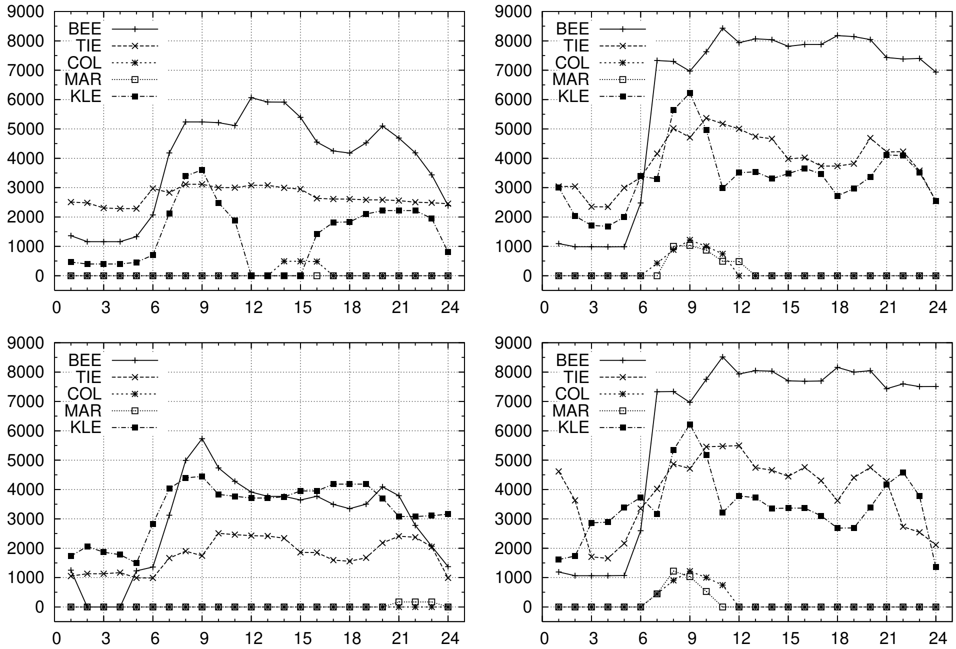

FIGURE 9. Optimal discharge flows into the southern uptown at BEE, TIE, COL, MAR, and KLE (m^3/h). Scenarios 1 (top left), 2 (top right), 3 (bottom left), and 4 (bottom right).

Since the behavior of the entire network is much too complex to visualize, we focus on a selected area in the southern uptown. This area is mainly served by the two waterworks Beelitzhof (BEE) and Tiefwerder (TIE), and it contains three pumping stations: Columbiadamm and Marienfelde (COL and MAR, with tanks), and Kleistpark (KLE, without tank). Note that the GEG differences (at Spandau and Tegel) and the nighttime reduction of the electricity price (at Stolpe) occur far from the area of interest; nevertheless we will see effects on the optimal operation schedules.

Figure 8 displays the raw water production at waterworks BEE and TIE, and the tank inflows at pumping stations COL and MAR. We observe that the raw water production is quite steady, as desired. Production is low during nighttime and high during daytime at almost constant levels. The slopes in between are also constant, showing that the gradient constraint (10) is binding. In scenarios 1 and 3 (normal demand) we have brief transitions between long periods with constant levels, and in scenarios 2 and 4 (high demand) we have a long nighttime transition and a brief constant daytime period. The two waterworks are always active in either case. Under normal demand, only one pumping station (COL) fills its tank during a brief period (either before midnight or in the early morning, depending on the GEG), whereas heavier nightly tank inflow and an additional late-afternoon inflow occur at both COL and MAR under high demand. With reduced GEG, both BEE and TIE produce significantly less water than in the reference case. Reducing the nighttime electricity price at the distant waterworks Stolpe has no visible effect here.

Figure 9 displays the outlet flow rates to the southern uptown at waterworks BEE and TIE, and at pumping stations COL, MAR, and KLE. In the reference case (normal demand), the outflow at TIE varies only slightly whereas BEE roughly follows the demand profile and KLE is under heavy load during the morning and evening peaks. Pumping station COL contributes a small share between the peak times. In scenario 2 (high demand) the behavior is totally different. Both BEE and TIE are under heavy load during daytime and still active at nighttime, while both COL and MAR feed the network only during the

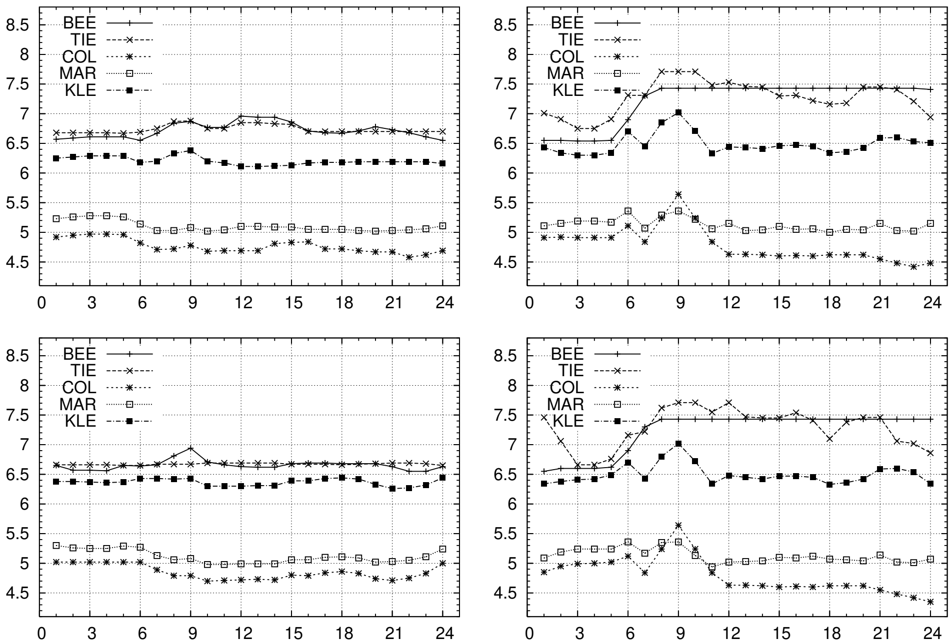

FIGURE 10. Optimal outlet pressures into the southern uptown at BEE, TIE, COL, MAR, and KLE (bar). Scenarios 1 (top left), 2 (top right), 3 (bottom left), and 4 (bottom right).

morning peak. Pumping station KLE works continuously during day and night, supplying a substantial share of water from a neighboring pressure zone where plants with high capacity and high efficiency are located. This effect is even more pronounced with reduced GEG at Spandau and Tegel (scenario 3), where KLE becomes the main source in compensating for the reduced production at BEE and TIE. Variable electricity costs result in lower nighttime supply from KLE and increased supply from TIE.

Figure 10 displays the outlet pressures at waterworks BEE and TIE, and at pumping stations COL, MAR, KLE. Under normal demand we observe only slight pressure variations, as desired. Note that pumping stations COL and MAR reach their maximal pressures during nighttime, although they are not pumping. The reason is that consumption is low, and hence there is very little pressure loss from the waterworks outlets to the customers. Under high demand there are substantial variations, especially before and during the morning peak, when the pressures reach their maximal values. Reducing the GEG or electricity price does not result in significant differences, except for higher nighttime pressure at TIE and lower pressure at KLE in scenario 4, corresponding to altered pump operation.

Figure 11 displays the tank filling levels at waterworks BEE and TIE, and at pumping stations COL and MAR. Under normal demand, the filling level at TIE is almost constant, and the tank is deflated very slightly during daytime. The tank at BEE is filled during peak times and deflated in between. In the reference case the tank at COL is full most of the time and is deflated during the evening peak, while the filling level at MAR remains constant. With reduced GEG (scenario 3) the level at COL remains constant while the tank at MAR shows a insignificant deflation during nighttime. The slight variations are partly caused by the constant electricity prices. Another reason is that the potential energy of the water is greater when the tanks are full, which reduces the power consumption of the outlet pumps. Under high demand, the tanks at BEE and TIE are operated as in scenario 1 but with somewhat greater deflation, while the tanks at COL and MAR are both substantially

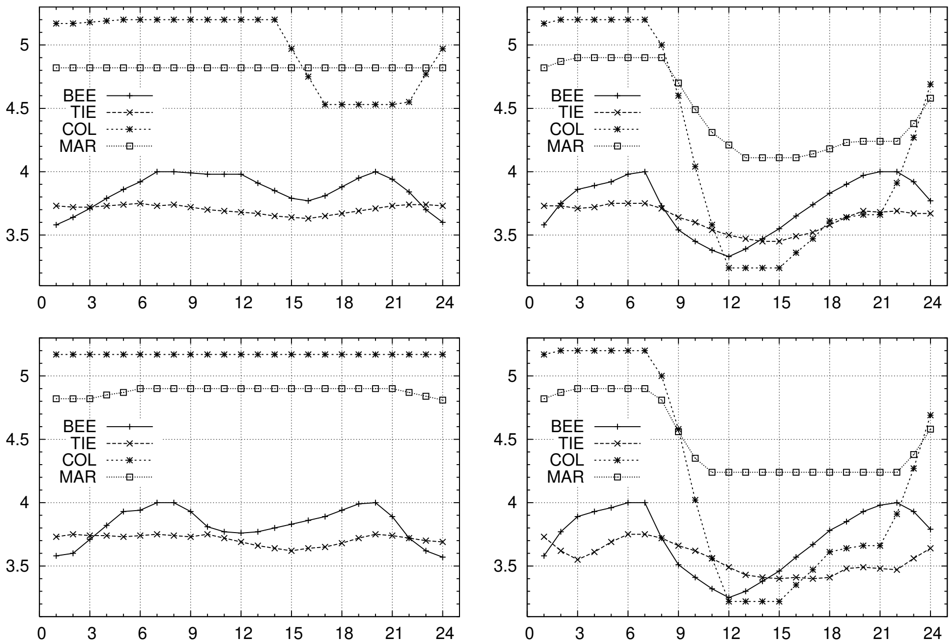

FIGURE 11. Optimal tank filling levels at BEE, TIE, COL, MAR (m). Scenarios 1 (top left), 2 (top right), 3 (bottom left), and 4 (bottom right).

deflated during daytime. This holds irrespective of the reduced nighttime electricity price which, however, causes permanently lower filling levels at TIE.

6. SUMMARY

We have presented a method for network-wide operative planning in pressurized water distribution networks that is practically applicable to large networks and under a wide range of operating conditions. An optimization module implementing our approach is integrated into the operational control system at Berliner Wasserbetriebe where it is used for the daily planning. Such an integration is emphasized in [51] as *the "hook" that interests the city water managers in trusting and, ultimately, using the system.* Notwithstanding this correct assessment, carefully dovetailed optimization models and numerical methods are essential in obtaining meaningful results, given the enormous complexity of the planning problem. Apart from sub-model approximations, convergence acceleration techniques, and the like, our approach features a network reduction strategy whose tradeoff between accuracy and numerical effort can be adjusted via a scalar parameter. It also features *smooth* minimum up and down time constraints which, in combination with pump aggregation, enable us to handle pump switching without introducing integral decision variables. Individual pump schedules are obtained in a post-processing step by solving separate mixed-integer NLP models (MINLP) *locally* at each outlet, with flows and pressures given by the network-wide NLP solution. The degree of detail for optimization in Berlin is mainly limited by what can be achieved in reasonable response time (up to 30 minutes) on affordable hardware (a PC workstation). From the modeling side, direct extensions to network-wide mixed-integer optimization as well as detailed component models are already available [6]. This allows for more accurate optimization as soon as faster hardware or improved algorithms become available. Using the current NLP model, further gains in efficiency may likely be obtained by developing custom sparse solvers based on similar techniques as in [19, 49], to exploit the rich sparse structure induced by the network model and time discretization.

References

[1] J. H. Andersen, R. S. Powell, and J. F. Marsh, *Constrained state estimation with applications in water distribution network monitoring*, Int. J. Syst. Sci., 32 (2001), pp. 807–816.

[2] H. Y. Benson, D. F. Shanno, and R. J. Vanderbei, *Interior-point methods for nonconvex nonlinear programming: Complementarity constraints*, Technical Report ORFE 02-02, Princeton University, 2002.

[3] P. F. Boulos, Z. Wu, C.-H. Orr, M. Moore, P. Hsiung, and D. Thomas, *Optimal Pump Operation of Water Distribuion Systems Using Genetic Algorithm, H_2ONET – Users Guide*, MW Software INC., 2000.

[4] J. Burgschweiger, *Grundlagenermittlung zum Modul Optimierung innerhalb des LSW-Management-systems*. Internal Report, Berliner Wasserbetriebe, 2001.

[5] ———, *Optimierung der verteilten Wasserförderung in großen Rohrnetzen*. Internal Report, Berliner Wasserbetriebe, June 2002.

[6] J. Burgschweiger, B. Gnädig, and M. C. Steinbach, *Optimization models for operative planning in drinking water networks*, ZIB Report ZR-04-48, Zuse Institute Berlin, 2004.

[7] R. H. Byrd, N. I. M. Gould, J. Nocedal, and R. A. Waltz, *An algorithm for nonlinear optimization using linear programming and equality constrained subproblems*, Math. Program., Ser. B, 100 (2004), pp. 27–48.

[8] R. H. Byrd, J. Nocedal, and R. A. Waltz, *Feasible interior methods using slacks for nonlinear optimization*, Comput. Optim. Appl., 26 (2003), pp. 35–61.

[9] E. K. Can and M. H. Houck, *Real-time reservoir operations by goal programming*, J. Water Resour. Plng. Mgmt., (1984), pp. 297–309.

[10] P. Carentier and G. Cohen, *Applied mathematics in water supply networks management*, Automatica, (1993), pp. 1215–1250.

[11] G. Cembrano, G. Wells, J. Quevedo, R. Perez, and R. Argelaguet, *Optimal control of a water distribution network in a supervisory control system*, Control Engineering Practice, (2000), pp. 1177–1188.

[12] R. G. Cembrowicz, *Steuerungsoptimierung eines Wasserversorgungssystems*, GWF – Wasser/Abwasser, 131 (1990), pp. 550–562.

[13] C. M. Chin and R. Fletcher, *On the global convergence of an SLP-filter algorithm that takes EQP steps*, Math. Program., 96 (2003), pp. 161–177.

[14] D. Cohen, U. Shamir, and G. Sinai, *Optimal operation of multi-quality water supply systems – II: The Q-H model*, Engineering Optimization, (2000), pp. 687–719.

[15] B. Coulbeck, M. Brdys, C. H. Orr, and J. P. Rance, *A hierarchical approach to optimized control of water distribution systems. I: Decomposition*, Optim. Control Appl. Methods, 9 (1988), pp. 51–61.

[16] ———, *A hierarchical approach to optimized control of water distribution systems. II: Lower-level algorithm*, Optim. Control Appl. Methods, 9 (1988), pp. 109–126.

[17] D. de Wolf and Y. Smeers, *The gas transmission problem solved by an extension of the simplex algorithm*, Management Sci., 46 (2000), pp. 1454–1465.

[18] A. Diba, P. W. F. Louie, and W. W.-G. Yeh, *Planned operation of large-scale water distribution system*, J. Water Resour. Plng. Mgmt., (1995), pp. 260–269.

[19] K. Ehrhardt and M. C. Steinbach, *KKT systems in operative planning for gas distribution networks*, Proc. Appl. Math. Mech., 4 (2004), pp. 606–607.

[20] ———, *Nonlinear optimization in gas networks*, in Modeling, Simulation and Optimization of Complex Processes, H. G. Bock, E. Kostina, H. X. Phu, and R. Rannacher, eds., Berlin, 2005, Springer, pp. 139–148.

[21] A. T. Ernst, *Continuous-time quadratic cost flow problems with applications to water distribution networks*, J. Aust. Math. Soc., Ser. B, 37 (1996), pp. 530–548.

[22] R. Fletcher and E. S. de la Maza, *Nonlinear programming and nonsmooth optimization by successive linear programming*, Math. Program., 43 (1989), pp. 235–256.

[23] R. Fletcher and S. Leyffer, *Solving mathematical programs with complementary constraints as nonlinear programs*, Optim. Methods Software, 19 (2004), pp. 15–40.

[24] *GAMS – A Users Guide*, Redwood City, 1988.

[25] B. Gnädig and M. C. Steinbach, *Betriebsoptimierung der Berliner Trinkwasserversorgung*. Zuse Institute Berlin, 2003. Study for ABB Utilities GmbH, Mannheim.

[26] ———, *Betriebsoptimierung der Berliner Trinkwasserversorgung mit Gesamtnetzmodell*. Zuse Institute Berlin, 2004. Study for ABB Utilities GmbH, Mannheim.

[27] M. Gugat, *Boundary controllability between sub- and supercritical flow*, SIAM J. Control Optim., 42 (2003), pp. 1056–1070.

[28] M. Gugat, G. Leugering, K. Schittkowski, and E. J. P. G. Schmidt, *Modelling, stabilization, and control of flow in networks of open channels*, in Online Optimization of Large Scale Systems, M. Grötschel, S. O. Krumke, and J. Rambau, eds., Springer, Berlin, 2001, pp. 251–270.

[29] F. Guhl, *Gestion optimale des réseaux d'eau potable*, PhD thesis, L'Université Louis Pasteur, 1999.

[30] P. Hackländer, *Integrierte Betriebsplanung von Gasversorgungssystemen*, Verlag Mainz, Wissenschaftsverlag, Aachen, 2002.

[31] C. T. HANSEN, K. MADSEN, AND H. B. NIELSEN, *Optmization of pipe networks*, Math. Program., Ser. B, 52 (1991), pp. 45–58.
[32] R. KLEMPOUS, J. KOTOWSKI, J. NIKODEM, AND J. ULASIEWICZ, *Optimization algorithms of operative control in water distribution systems*, J. Comput. Appl. Math., 84 (1997), pp. 81–99.
[33] C. D. LAIRD, L. T. BIEGLER, B. G. VAN BLOEMEN WAANDERS, AND R. A. BARTLETT, *Time dependent contamination source determination for water networks using large scale optimization*, tech. rep., Carnegie Mellon University and Sandia National Labs, 2003.
[34] G. LEUGERING AND E. J. P. G. SCHMIDT, *On the modelling and stabilization of flows in networks of open canals*, SIAM J. Control Optim., 41 (2002), pp. 164–180.
[35] A. MARTIN AND M. MÖLLER, *Cutting planes for the optimization of gas networks*, in Modeling, Simulation and Optimization of Complex Processes, H. G. Bock, E. Kostina, H. X. Phu, and R. Rannacher, eds., Berlin, 2005, Springer, pp. 307–329.
[36] S. MIJAOKA AND M. FUNABASHI, *Optimal control of water distribution systems by network flow theory*, IEEE Trans. Automat. Contr., (1984), pp. 303–311.
[37] M. MÖLLER, *Mixed Integer Models for The Optimisation of Gas Networks in the Stationary Case*, PhD thesis, Technische Universität Darmstadt, 2004.
[38] D. M. MURRAY AND S. J. YAKOWITZ, *Constrained differential dynamic programming and its application to multireservoir control*, Water Resources Research, 15 (1979), pp. 223–235.
[39] C. H. ORR, M. A. PARKER, AND S. T. TENNANT, *Implementation of on-line control scheme for city water system*, J. Water Resour. Plng. Mgmt., (1990), pp. 708–726.
[40] V. V. OSTAPENKO AND A. I. PAVLYGIN, *Dynamic network flows for generalized Kirchhoff law*, Cybern. Syst. Anal., 32 (1996), pp. 309–397.
[41] M. PAPAGEORGIOU, *Optimal control of generalized flow networks*, in System Modelling and Optimization, Proc. 11th IFIP Conf., Copenhagen 1983, vol. 59 of Lect. Notes Control Inf. Sci., Berlin, 1984, pp. 373–382.
[42] A. U. RAGHUNATHAN AND L. T. BIEGLER, *Interior point methods for mathematical programs with complementarity constraits (MPCCs)*, tech. rep., Carnegie Mellon University, 2003.
[43] K. REINISCH, C. THÜMMLER, AND S. HOPFGARTEN, *Hierarchical on-line control algorithm for repetitive optimization with predicted environment and its application to water management problems*, Syst. Anal., Modelling Simulation, 1 (1984), pp. 263–280.
[44] L. A. ROSSMAN, *EPANET Users Guide*, US Environmental Protection Agency, Cincinnati, 1994.
[45] A. B. A. SAKARYA AND L. W. MAYS, *Optimal operation of water distribution pumps considering water quality*, J. Water Resour. Plng. Mgmt., (2000), pp. 210–220.
[46] S. SCHOLTES, *Convergence properties of a regularization scheme for mathematical programs with complementarity constraints*, SIAM J. Optim., 11 (2001), pp. 918–936.
[47] H. D. SHERALI, S. SUBRAMANIAN, AND G. V. LOGANATHAN, *Effective relaxations and partitioning schemes for solving water distribution network design problems to global optimality*, J. Glob. Optim., 19 (2001), pp. 1–26.
[48] O. STEIN, J. OLDENBURG, AND W. MARQUARDT, *Continuous reformulations of discrete-continuous optimization problems*, Comput. Chem. Eng., 28 (2004), pp. 1951–1966.
[49] M. C. STEINBACH, *On PDE solution in transient optimization of gas networks*, J. Comput. Appl. Math. Accepted for publication.
[50] Y.-H. SUN, W. W.-G. YEH, N.-S. HSU, AND P. W. F. LOUIE, *Generalized network algorithm for water-supply-system optimization*, J. Water Resour. Plng. Mgmt., (1995), pp. 392–398.
[51] R. L. WILSON, B. T. REELY, AND M. COX, *The water resource management system (WREMS): Linking data management and operational optimization*, Ann. Oper. Res., 72 (1997), pp. 105–124.
[52] B. YOUNG, *Analysis and optimisation of looped water distribution networks*, J. Aust. Math. Soc., Ser. B, 41 (2000), pp. 508–526.
[53] U. ZESSLER AND U. SHAMIR, *Optimal operation of water distribution systems*, J. Water Resour. Plng. Mgmt., (1989), pp. 737–751.

JENS BURGSCHWEIGER, BERLINER WASSERBETRIEBE, NETZ- UND ANLAGENBAU, 10864 BERLIN, GERMANY
E-mail address: jens.burgschweiger@bwb.de
URL: http://www.bwb.de

BERND GNÄDIG, DÜSSELDORF, GERMANY
E-mail address: bernd.gnaedig@gmx.de

MARC C. STEINBACH, ZUSE INSTITUTE BERLIN (ZIB), DEPARTMENT OPTIMIZATION, TAKUSTR. 7, 14195 BERLIN, GERMANY
E-mail address: steinbach@zib.de
URL: http://www.zib.de/steinbach